JACS
JOURNAL OF THE AMERICAN CHEMICAL SOCIETY
Article
pubs.acs.org/JACS

A Study of the Mechanism of the Hydrogen Evolution Reaction on Nickel by Surface Interrogation Scanning Electrochemical Microscopy

Zhenxing Liang,[†] Hyun S. Ahn,[*,‡] and Allen J. Bard[*,†]

[†]Center for Electrochemistry, Department of Chemistry, The University of Texas at Austin, Austin, Texas 78712, United States
[‡]Department of Chemistry, Yonsei University, 50 Yonsei-ro, Seodaemun-gu, Seoul 03722, Korea

Supporting Information

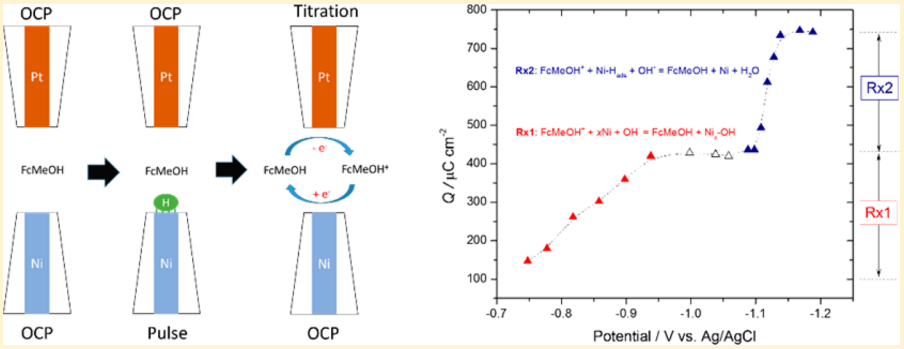

ABSTRACT: The hydrogen evolution reaction (HER) on Ni in alkaline media was investigated by scanning electrochemical microscopy under two operating modes. First, the substrate generation/tip collection mode was employed to extract the "true" cathodic current associated with the HER from the total current in the polarization curve. Compared to metallic Ni, the electrocatalytic activity of the HER is improved in the presence of the low-valence-state oxide of Ni. This result is in agreement with a previous claim that the dissociative adsorption of water can be enhanced at the Ni/Ni oxide interface. Second, the surface-interrogation scanning electrochemical microscopy (SI-SECM) mode was used to directly measure the coverage of the adsorbed hydrogen on Ni at given potentials. Simulation indicates that the hydrogen coverage follows a Frumkin isotherm with respect to the applied potential. On the basis of the combined analysis of the Tafel slope and surface hydrogen coverage, the rate-determining step is suggested to be the adsorption of hydrogen (Volmer step) in the investigated potential window.

INTRODUCTION

Significant progress has been achieved to develop active catalysts for the hydrogen evolution reaction (HER) in recent years.[1,2] One big step worth noting is the rational design of the bifunctional catalyst,[3] which has been proposed by Markovic et al.[1,4] The optimal HER catalyst depends on the properties of the metal/metal oxide interface at which the adsorption of the reactive hydrogen intermediates occurs on the Pt group metal and the sorption of -OH happens on the hydrophilic metal oxide.[5,6] Following this approach, Tang et al.[7] deposited Pt nanowires onto single-layered nicked hydroxide, yielding good electrocatalytic activities for the HER.

Ni and its alloys have been widely studied as excellent electrocatalysts for the HER in alkaline media;[8] however, the mechanism of reaction has not been well understood. One reason is the lack of a reliable in situ method to directly measure the coverage of the hydrogen intermediate at the electrode/electrolyte interface. Efforts have been devoted to exploring various electrochemical methods such as galvanostatic charging[9,10] and open circuit potential decay[11,12] to determine the coverage of hydrogen. However, the results were imperfect because of inherent issues with the techniques or inappropriate assumptions in the data fitting.[9,11,12] In comparison, surface-interrogation scanning electrochemical microscopy (SI-SECM), developed in our group, is a unique and direct method to measure the coverage of the active adsorbates such as -H_{ads}, -OH_{ads}, -CO_{ads} on the surface of the electrode.[13−21]

Another key issue in the mechanistic study is that Ni is oxidized in aqueous media; therefore, in collecting the polarization curve, the "true" HER current is not easily differentiated from the overlapping electrochemical reduction of the oxide, which further complicates the correlation between the intrinsic activity and the adsorption energy.[22] As such, special care should be taken in collecting and analyzing the polarization curve of the HER. Leonard[16] developed a method to differentiate the HER current from the total current using the substrate generation/tip collection (SG/TC) SECM in which hydrogen generated on the metal electrode of interest can be fully collected and accurately analyzed.

Received: January 11, 2017
Published: March 9, 2017

ACS Publications © 2017 American Chemical Society

DOI: 10.1021/jacs.7b00279
J. Am. Chem. Soc. 2017, 139, 4854−4858

By using the aforementioned methods, the Ni and Pt ultramicroelectrodes (UME) were fabricated and used as the substrate and tip electrodes, respectively, in the SECM experiments. The cathodic current due to the HER was collected with SG/TC SECM, and the coverage of -H_{ads} was determined by titration using a ferrocenemethanol mediator in the SI-SECM experiments, that is, the tip-generated ferrocenium reacted with adsorbed hydrogen on the Ni substrate surface. The rate-determining step of the HER was then explored based on Tafel analysis and the -H_{ads} coverage. To the best of our knowledge, this is the first report to accurately collect the "true" current of the HER and directly measure the coverage of adsorbed hydrogen on the Ni electrode, which ensures the validity of the mechanistic analysis. It also provides evidence of the electrocatalysis of the Ni hydroxide.

RESULTS AND DISCUSSION

Effect of Ni Oxide on HER. Ni hydroxide was generated by an in situ electrochemical method in which the chemical state was controlled by varying the upper limit potential (E_{ul}) in a cyclic voltammetry (CV) scan. The effect on the HER is shown in Figure 1. The cathodic current at a given potential

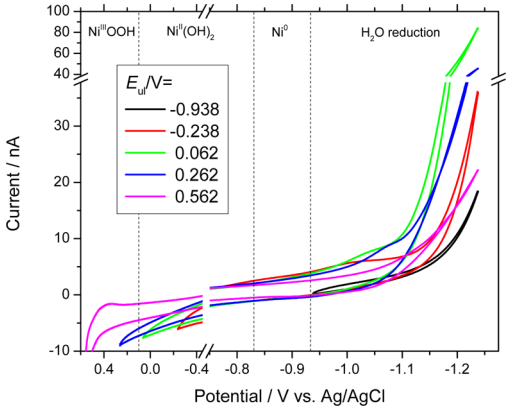

Figure 1. Cyclic voltammograms of the Ni UME (a = 12.5 μm) at different upper limit potentials (E_{ul}).

continuously increased when E_{ul} increased from −0.938 to 0.062 V, which decreased however with a further increase in E_{ul}. The generation of low-valence state Ni oxide can facilitate the HER on Ni, as proposed by Markovic.[1,4] However, the cathodic current originates from the reduction reactions of both water and Ni oxide. The overlapped reduction of oxide makes the above analysis on the HER unreliable,[5] and the "true" cathodic current of the HER has to be extracted from the i-E curve. For this goal to be achieved, the SG/TC mode of SECM was applied to differentiate the cathodic current of the HER, as shown in Figure 2. Under this working mode, the potential of the Pt tip was set at −0.6 V, which ensures the fast and complete oxidation of any hydrogen evolved from the Ni substrate. As such, the anodic current of the Pt tip can be used as the "true" current of the HER on the Ni substrate. Figure 2a shows that the current of the Ni substrate is much larger than that of the Pt tip, confirming that the cathodic reduction of the Ni oxide cannot be neglected. Such behavior explains why the literature-reported polarization curves and Tafel analyses may be unreliable.[8,23−26] In addition, the generated hydrogen can diffuse into the bulk Ni, which cannot be detected by the probe and may contribute to the larger cathodic current on the substrate electrode.

Panels b and c in Figures 2 present the cyclic voltammograms on the Ni substrate at various upper limit potentials and the corresponding anodic current detected on the Pt tip. First, a broad cathodic shoulder is observed at approximately −1.0 V, which becomes more pronounced with increasing upper limit potential. In comparison, hydrogen detected on the Pt tip is negligible in this potential region. This overlapping shoulder originates from the reduction of the Ni oxide that was generated at higher potentials during the scan. Second, the electrocatalytic activity of the HER shows a volcano-shape relationship (see Figure S2) with respect to the upper limit potential and peaks at E_{ul} = 0.062 V. In the left branch (E_{ul} < 0.062 V), the electrocatalytic activity improves with increasing upper limit potential. This can be attributed to the adsorption of the hydroxyl ions and consequent formation of low-valence state oxides (mostly $Ni(OH)_2$, $E^{o}_{Ni(OH)2/Ni}$= −0.83 V[27]) on the surface, which favors the dissociative adsorption of water, namely, the Volmer step (eq 1).[1,4,5] In the right branch, a further increase in the upper limit potentials (E_{ul} > 0.062 V) decreases the activity of the HER. At high E_{ul}, coverage by the excess low-valence state oxide and the presence of the high-valence state oxide ($E^{o}_{NiOOH/Ni(OH)2}$ = 0.17 V[27]) hinder the electron transfer at the interface and the adsorption of hydrogen on Ni sites. As a result, the electrocatalytic activity of the HER decreases in this process.

$$\text{Volmer step: } H_2O + Ni + Ni(OH)_2 + e^- \rightarrow Ni - H_{ad} + Ni(OH)_2\text{-}OH^-_{ad} \quad (1)$$

In addition, a hysteresis loop in the HER current is observed and becomes more pronounced upon increasing E_{ul} > 0.162 V. Such a hysteresis loop can be rationalized by considering the coverage of oxide on the surface. In the negative potential scan, the generated oxide at high potentials cannot be completely stripped off, which disrupts hydrogen adsorption and results in a lower activity. In the positive scan, the oxide is slowly reduced, and hence, both the valence state and coverage of the oxide yield less negative effects on the HER. For further support for this analysis, the effect of cycling was investigated in the potential scans. Figure 2d shows the result of sequential curves at E_{ul} of 0.062 and 0.562 V. The current remains unchanged at E_{ul} = 0.062 V, whereas it declines to a large extent at E_{ul} = 0.562 V. Such a dramatic decrease originates from the oxide not being completely reduced but accumulating during the continuous scans.

Coverage of Adsorbed Hydrogen Determined by SI-SECM. The adsorbed hydrogen on the Ni electrode substrate at given potentials was found by bringing it to a given test potential, then at open circuit, rapidly titrating with ferrocenemethanol$^+$ ($FcMeOH^+$) generated at the tip: the SI-SECM method, titration curve shown in Figure 3a (see also Figure S3). Detailed procedures for the experimental preparation are given in the Supporting Information, see also refs 13−21 for variations in the SI-SECM. Two charge plateaus can be observed in the plot. First, the charge continuously increases as the potential becomes more negative, which then reaches an inflection point at −0.92 V. This charge originates from the titration reaction between the titrate $FcMeOH^+$ and metallic Ni. The coverage of the Ni oxide continues to decrease as the potential becomes more negative, and hence, the charge of surface metal Ni titrated by $FcMeOH^+$ increases in the

DOI: 10.1021/jacs.7b00279
J. Am. Chem. Soc. 2017, 139, 4854−4858

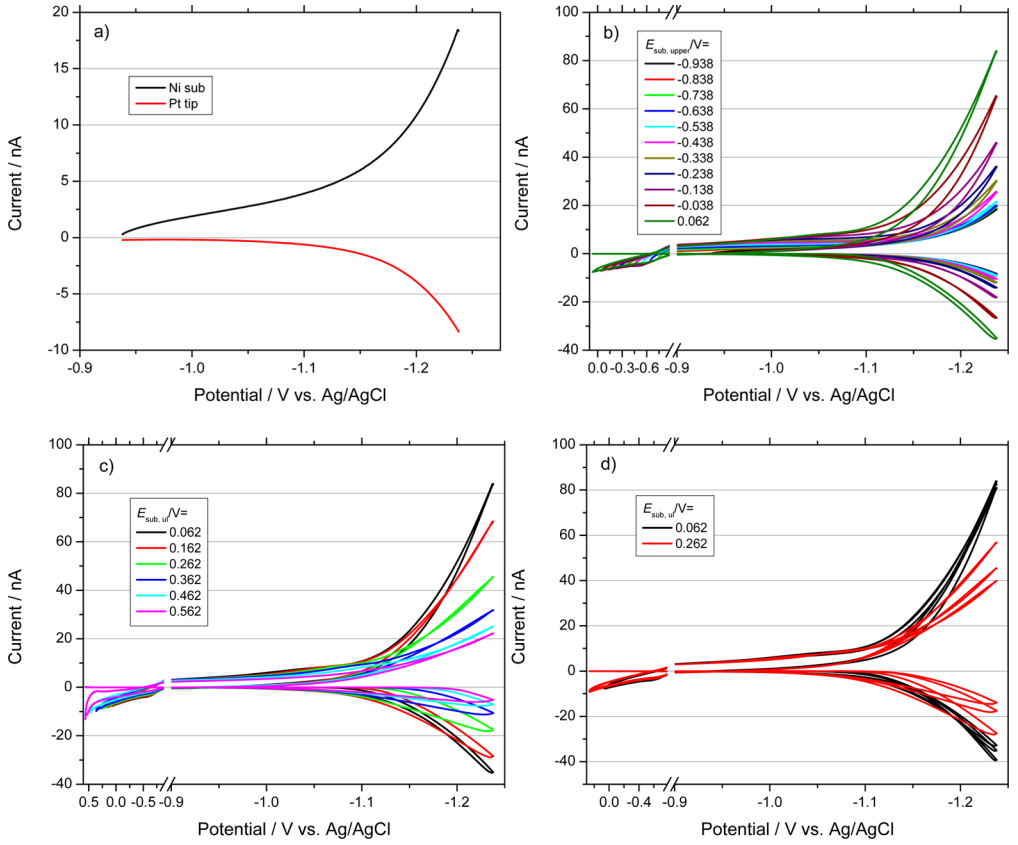

Figure 2. SG/TC mode of SECM results of the HER in 1.0 mM FcMeOH + 0.010 M KOH solution. Substrate: Ni UME (a = 12.5 μm), v = 50 mV s^{-1}; tip: Pt UME (a = 12.5 um), E_{tip} = −0.6 V; approach distance (L): 2.0 μm.

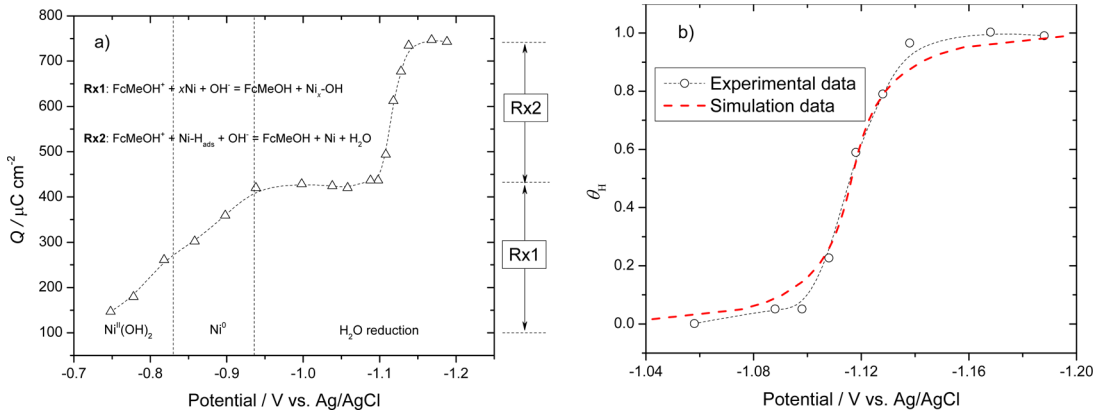

Figure 3. Plot of charge density (a) and coverage of adsorbed hydrogen (b) vs E_{sub} constructed from interrogation transients on Ni in 0.010 M KOH. The simulation parameters related to the Frumkin isotherm $e^{F(E^{0'}-E)/RT}a_{H_2O} = \frac{\theta}{1-\theta}e^{-g'\theta}$, where F = 96485 C mol^{-1}, R = 8.315 J K^{-1} mol^{-1}, T = 298.15 K, $E^{0'}$ = −1.155 V, a_{H_2O} = 1; g' = 3, and θ = 0.2−0.8.

process. At potentials of −0.92 to −1.1 V, the surface is basically in the metal state, and as a result, the charge remains unchanged. As the potential further decreases to −1.15 V, a second inflection point is observed with Q = 315 μC cm^{-2} (subtracting the baseline charge density of approximately 435 μC cm^{-2} of the Ni surface at −1.0 V from the charge density of approximately 750 μC cm^{-2} near the plateau for Ni−H_{ads} at −1.15 V). The charge originates from the reaction between the $FcMeOH^+$ and the adsorbed hydrogen on Ni. As such, this inflection point corresponds to $Q_{\theta=1,H}$ with a roughness factor of 1.21. The coverage of adsorbed hydrogen is then calculated and plotted in Figure 3b. At potentials more positive than −1.1 V, the coverage of adsorbed hydrogen is negligible, indicating that the adsorption of hydrogen is slow. With the potential becoming more negative, the coverage of hydrogen increases and reaches unity at −1.14 V. The simulation reveals that the coverage follows a Frumkin isotherm with g' = 3, indicating that the interaction between the neighboring adsorbed species is attractive.[19,28]

Tafel Analysis and Kinetics Parameters. Figure 4 shows the tafel plot of the HER at different upper limit potentials. All of the curves basically yield the same tafel slope of

DOI: 10.1021/jacs.7b00279
J. Am. Chem. Soc. 2017, 139, 4854−4858

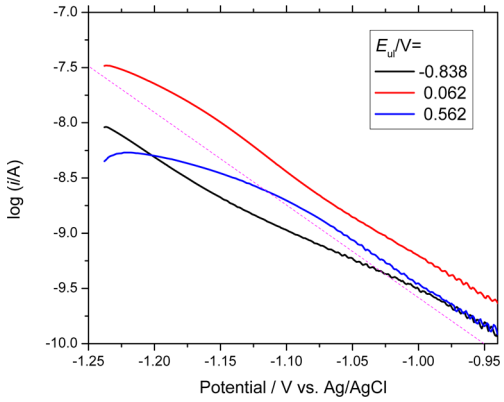

Figure 4. Tafel plot of the hydrogen evolution reaction on the Ni electrode.

approximately 120 mV dec^{-1}, revealing that the rate-determining step (rds) involves a one-electron transfer. This could be either a Volmer (eq 1) or Heyrovsky (eq 2) step. As mentioned above, the adsorption of hydrogen occurs slowly in the potential range of −0.95 to −1.1 V. As such, the Volmer step is suggested to be the rds of the HER in this potential range. It is thus understandable why the presence of nickel oxide can hasten the Volmer step and thereby the HER, as shown by eq 1. For it to be made clearer, the kinetics parameters are calculated by fitting the polarization curve (see Figure S4), as shown in Table 1. The standard reaction rate

Table 1. Kinetics Parameters of the HER on the Ni Electrode at Different Upper Limit Potentials

E_{ul}/V	$j^0 \times 10^5$/A cm^{-2}	$k^o \times 10^9$/cm s^{-1}
−0.838	2.66	5.01
−0.738	2.74	5.16
−0.538	2.79	5.27
−0.438	2.86	5.39
−0.338	2.95	5.55
−0.238	3.31	6.23
−0.138	3.69	6.96
−0.038	4.09	7.72
0.062	4.33	8.15

constant (k^0) continuously increases from 5.0 to 8.1 × 10^{-9} cm s^{-1} when the upper limit potential increases from −0.838 to 0.062 V, further confirming the above analysis on the rds.

$$\text{Heyrovsky step: Ni-H}_{ad} + H_2O + e^- \rightarrow Ni + H_2 + OH^- \quad (2)$$

CONCLUSIONS

In this work, SECM was used to differentiate the polarization curve of the hydrogen evolution reaction and measure the surface coverage of the adsorbed hydrogen on Ni in alkaline media. The mechanism of the HER was investigated, and the salient findings include the following: (i) The presence of the surface oxide of low-valence state promotes the HER, e.g., dissociative adsorption of water and thus the Volmer step. (ii) The coverage of adsorbed hydrogen follows a Frumkin isotherm with respect to the given potential. (iii) The rds is found to be the Volmer step in the investigated potential range.

EXPERIMENTAL

General. All solutions were prepared using Milli-Q deionized water (18.2 MΩ cm, 4 ppb total oxidizable carbon). Potassium hydroxide (98%, Fisher) and ferrocenemethanol (97%, Sigma-Aldrich) were used as received. Platinum (99.99%) and nickel wires (99.98%) of 25 μm diameter were purchased from Goodfellow (Devon, PA). The metal wire was used to fabricate the ultramicroelectrode (UME) as described elsewhere.[29] All electrodes used in this study had an RG (RG = [radius of the electrode plus the glass sheath]/[radius of the electrode]) of ∼1.5 and were polished with alumina paste on microcloth pads prior to use. For all electrochemical measurements, an Ag/AgCl (1.0 M KCl) reference electrode and a gold wire counter electrode were used. The redox mediator used in this study was 1.0 mM ferrocenemethanol in the 0.010 M KOH aqueous solution (pH 12.0). All solution used in the electrochemical cell were thoroughly bubbled with Ar prior to experimentation and were kept under a humidified argon blanket.

Instrumentation. SECM experiments were conducted using a CHI920C SECM station bipotentiostat and its built-in software (CH Instruments; Austin, TX). Cyclic voltammetry (CV) was chosen as the detection technique in the SI-SECM experiments. The Pt tip and the Ni substrate electrodes (both 25 μm UME) were positioned at 2.0 μm from one another, a distance at which generation-collection efficiency was unity (refer to Supporting Information for details of electrode alignment and placement). For each data point collected, the Ni substrate was stepped to E_{sub} for a time t_{step} = 60 s followed by a step back to an open circuit. A rest time of 10 s was applied between generation and interrogation for the generated hydrogen to leave the tip−substrate gap. Then, cyclic voltammetry experiments were carried out at the tip electrode over a potential range between 0 and 0.5 V at a scan rate of 50 mV s^{-1}. The magnitude of the potential step applied on the substrate electrode was changed by 10 mV after each run.

ASSOCIATED CONTENT

Supporting Information

The Supporting Information is available free of charge on the ACS Publications website at DOI: 10.1021/jacs.7b00279.

SI-SECM alignment and approach, the relationship between HER current and the upper limit potential, titration curves, and kinetic parameters (PDF)

AUTHOR INFORMATION

Corresponding Authors

*ahnhs@yonsei.ac.kr

*ajbard@mail.utexas.edu

ORCID

Allen J. Bard: 0000-0002-8517-0230

Notes

The authors declare no competing financial interest.

ACKNOWLEDGMENTS

This work was financially supported by the National Science Foundation (CHE-1405248) and the Welch Foundation (F-0021). Z.X.L. is grateful for the support of the National Natural Science Foundation of China (21676106, 21476087).

REFERENCES

(1) Subbaraman, R.; Tripkovic, D.; Strmcnik, D.; Chang, K. C.; Uchimura, M.; Paulikas, A. P.; Stamenkovic, V.; Markovic, N. M. *Science* **2011**, *334*, 1256.

(2) Wang, C. M.; Bai, S.; Xiong, Y. J. *Chin. J. Catal.* **2015**, *36*, 1476.

(3) Long, G. F.; Li, X. H.; Wan, K.; Liang, Z. X.; Piao, J. H.; Tsiakaras, P. *Appl. Catal., B* **2017**, *203*, 541.

(4) Subbaraman, R.; Tripkovic, D.; Chang, K. C.; Strmcnik, D.; Paulikas, A. P.; Hirunsit, P.; Chan, M.; Greeley, J.; Stamenkovic, V.; Markovic, N. M. *Nat. Mater.* **2012**, *11*, 550.

DOI: 10.1021/jacs.7b00279
J. Am. Chem. Soc. 2017, 139, 4854−4858

(5) Zhou, Y. G.; Rees, N. V.; Compton, R. G. *Phys. Chem. Chem. Phys.* **2013**, *15*, 761.
(6) Mao, Y.; Chen, J. F.; Wang, H. F.; Hu, P. *Chin J. Catal.* **2015**, *36*, 1596.
(7) Yin, H.; Zhao, S.; Zhao, K.; Muqsit, A.; Tang, H.; Chang, L.; Zhao, H.; Gao, Y.; Tang, Z. *Nat. Commun.* **2015**, *6*, 6430.
(8) Ledendecker, M.; Clavel, G.; Antonietti, M.; Shalom, M. *Adv. Funct. Mater.* **2015**, *25*, 393.
(9) Divisek, J. *J. Electroanal. Chem. Interfacial Electrochem.* **1986**, *214*, 615.
(10) Devanathan, M. A. V.; Selvaratnam, M. *Trans. Faraday Soc.* **1960**, *56*, 1820.
(11) Conway, B. E.; Bai, L.; Tessier, D. F. *J. Electroanal. Chem. Interfacial Electrochem.* **1984**, *161*, 39.
(12) Lasia, A.; Rami, A. *J. Electroanal. Chem. Interfacial Electrochem.* **1990**, *294*, 123.
(13) Rodriguez-Lopez, J.; Alpuche-Aviles, M. A.; Bard, A. J. *J. Am. Chem. Soc.* **2008**, *130*, 16985.
(14) Wang, Q.; Rodriguez-Lopez, J.; Bard, A. J. *J. Am. Chem. Soc.* **2009**, *131*, 17046.
(15) Rodriguez-Lopez, J.; Bard, A. J. *J. Am. Chem. Soc.* **2010**, *132*, 5121.
(16) Leonard, K. C.; Bard, A. J. *J. Am. Chem. Soc.* **2013**, *135*, 15890.
(17) Ahn, H. S.; Bard, A. J. *J. Am. Chem. Soc.* **2015**, *137*, 612.
(18) Ahn, H. S.; Bard, A. J. *Anal. Chem.* **2015**, *87*, 12276.
(19) Arroyo-Currás, N.; Bard, A. J. *J. Phys. Chem. C* **2015**, *119*, 8147.
(20) Ahn, H. S.; Bard, A. J. *J. Am. Chem. Soc.* **2016**, *138*, 313.
(21) Ahn, H. S.; Bard, A. J. *J. Phys. Chem. Lett.* **2016**, *7*, 2748.
(22) Quaino, P.; Juarez, F.; Santos, E.; Schmickler, W. *Beilstein J. Nanotechnol.* **2014**, *5*, 846.
(23) Correia, A. N.; Machado, S. A. S. *Electrochim. Acta* **1998**, *43*, 367.
(24) Fournier, J.; Menard, H.; Brossard, L. *J. Appl. Electrochem.* **1995**, *25*, 923.
(25) Franceschini, E. A.; Lacconi, G. I.; Corti, H. R. *Electrochim. Acta* **2015**, *159*, 210.
(26) Kibria, M. *Int. J. Hydrogen Energy* **1995**, *20*, 435.
(27) Beverskog, B.; Puigdomenech, I. *Corros. Sci.* **1997**, *39*, 969.
(28) Chun, J. H.; Ra, K. H.; Kim, N. Y. *J. Electrochem. Soc.* **2002**, *149*, E325.
(29) Bard, A. J.; Mirkin, M. V. *Scanning Electrochemical Microscopy*, 2nd ed.; CRC Press, 2012.

DOI: 10.1021/jacs.7b00279
J. Am. Chem. Soc. 2017, 139, 4854−4858